

П.О. Коробко¹, А.В. Кузьмов^{1,2}, М.Б. Штерн¹*Інститут проблем матеріалознавства ім. І.М. Францевича НАН України¹
Київський академічний університет²***МОДЕЛЮВАННЯ ПЛАСТИЧНОЇ ПОВЕДІНКИ ПОРИСТОГО МАТЕРІАЛУ ЗІ СТРУКТУРОЮ ІНВЕРСНОГО ОПАЛУ ПРИ ВЕЛИКИХ ДЕФОРМАЦІЯХ**

Шляхом скінчено-елементного моделювання на представницькому осередку досліджено процес незворотного пластичного деформування пористого матеріалу з інверсно-опаловою структурою аж до моменту, коли структура пор стає майже повністю закритою. Це є важливим для прогнозування збереження адсорбційних та хімічно-каталітичних функціональних властивостей інверсно-опалових матеріалів при експлуатації та обробці тиском. Виявилось, що структура інверсного опалу зберігає відкриту пористість навіть за досить великих деформацій. Встановлена суттєва розбіжність між інженерним критерієм текучості 0.2 % залишкової деформації та фізичною границею текучості.

Ключові слова: метаматеріали, інверсний опал, представницький осередок, пластична деформація, відкрита пористість, границя текучості.

P. Korobko, A. Kuzmov, M. Shtern

MODELING THE PLASTIC BEHAVIOR OF A POROUS MATERIAL WITH AN INVERSE OPAL STRUCTURE AT LARGE DEFORMATION

By means of finite element modeling on a representative cell, the process of irreversible plastic deformation of a porous material with an inverse opal structure was investigated up to the moment when the pore structure becomes almost completely closed. This is important for predicting the preservation of the adsorption and chemical-catalytic functional properties of inverse opal materials during operation and pressure treatment. It was found that the structure of inverse opal retains permeable porous structure even under fairly large deformations. A significant discrepancy was found between the engineering yield criterion of 0.2% residual strain and the physical yield point.

Keywords: metamaterials, inverse opal, unit cell, plastic deformation, permeable porous structure, yield limit.

Introduction.

With the development of materials production technologies, composite materials with a periodic ordered structure have recently begun to be distinguished into a separate class and called metamaterials [1]. Such metamaterials include, in particular, porous materials with an inverse opal structure [2, 3], which can have high adsorption [4], catalytic [5], photocatalytic [6], and capillary [7] properties. The structure of such porous materials is formed by filling the voids between the regular dense packing of spheres with some interparticle contacts with a substance. After that, the substance of densely packed spheres is removed from the composite material and a porous material with an inverse opal structure is obtained (Fig. 1 a). Subsequently, a coating of a certain thickness can be applied to this frame while maintaining the open pore structure (Fig. 1 b).

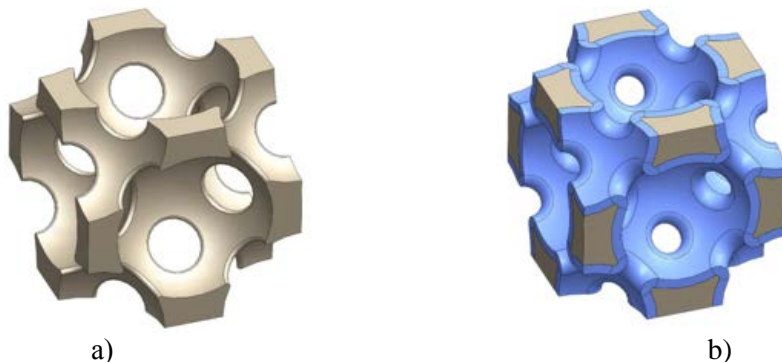


Fig. 1. Periodic structure of inverse opal a) without coating; b) with coating

In their previous works, the authors modeled the elastic [8] and plastic [9] properties of inverse opal structures, while the plasticity criterion, similar to work [2], was taken as the common engineering criterion of achieving 0.2% irreversible deformation. However, for such a highly porous material as inverse opal, it is also interesting to study its plastic behavior at much higher degrees of deformation than 0.2%. Therefore, the **aim** of this work was to study the plastic behavior of a porous material with an inverse opal structure at significant deformation. At the same time, by means of finite element modeling in the volume of a unit cell,

© П.О. Коробко, А.В. Кузьмов, М.Б. Штерн

deformation was studied up to the moment of contact of different edges of the pore surface, that is, in fact, until the moment when the pore structure loses permeability and becomes closed. Studying the issue of the transition of the structure type from open porosity to closed porosity is important for predicting the preservation of adsorption and chemical-catalytic functional properties. As in the previous works of the authors [8,9] and work [2], nickel was used as the material for both the initial inverse opal structure and the additional deposited layer. In this work, we will limit ourselves to the case of uniaxial compression of an inverse opal porous material, in particular for the purpose of comparing the physical yield point σ_T with the engineering criterion $\sigma_{0,2}$. The structure of inverse opal can be described by two parameters, which in this work were used as the porosity Θ and the thickness of the additionally deposited nickel layer.

Micromechanical averaging of the stress-strain state in inverse opal.

Due to symmetry, in the case where the XYZ coordinate system shown in Fig. 2 lacks shear components of macroscopic "effective" [10, 11] deformations, the cell will retain a rectangular shape during such deformation. Therefore, even under macroscopic uniaxial compressive loading along the Z axis (i.e., when σ_{zz} is the only non-zero component in the macroscopic "effective" stress tensor), the shape of the periodic cell will remain rectangular. Let's denote the dimensions of a rectangular cell h_x, h_y, h_z . Micromechanical boundary conditions [10, 11], which relate the stress-strain state in the cell volume to the "effective" strain ε_{zz} or stress σ_{zz} , in this case will take the form:

- The points of each wall continue to lie in a plane with the same normal $u_n^i - u_n^i = 0$
- For the upper wall, some fixed component of displacement is given $u_n^i = u_z^i = u_0 = \varepsilon_{zz} h_z$, and for the lower wall $u_n^i = u_z^i = 0$.

At the same time, knowing, as a result of solving the equilibrium equations with these boundary conditions, the resultant force P_z on the upper wall (which, according to the problem formulation, can only be in the Z direction), one can easily calculate the macroscopic stresses $\sigma_{zz} = P_z/S$ corresponding to u_0 and ε_{zz} , where S is the area of the upper wall of the rectangular cell. Due to symmetry, the simulation was carried out on a quarter of the periodic cell Fig. 2.

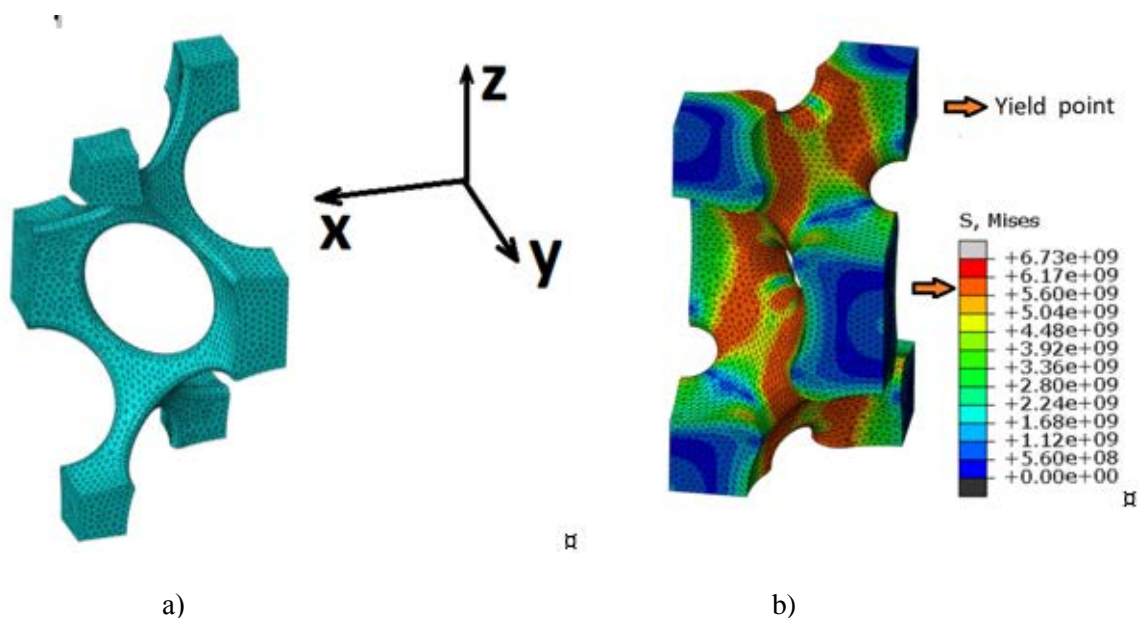


**Fig.2. Finite element modeling in the volume of a periodic unit cell:
a) finite element mesh; b) von Mises stress distribution**

It is worth noting that since in the boundary conditions there are restrictions only on the normal component of the velocity of the nodes on the walls of the cell, the tangential stresses on each of the walls, and accordingly the tangential components of the macroscopic "effective" stresses, will be zero. We also note that the finite element modeling software we used makes it possible to tie a certain component of the

movement of all points of the plane to the movement of some fixed point on it. And if the magnitude of such a displacement itself is not specified, then this displacement will take on such a value that the resultant force on this plane is zero. Thus, the absence of other components of the "effective" stress tensor except σ_{zz} is achieved.

By changing the sign of u_0 , one can go from uniaxial loading to uniaxial unloading, up to the moment when $\sigma_{zz} = 0$. At the same time, if during loading the frame material underwent irreversible plastic deformation, then at the moment of complete unloading, when $\sigma_{zz} = 0$, the magnitude of macroscopic deformations is $\varepsilon_{zz} = \varepsilon_{zz}^{pl} \neq 0$. This non-zero value of ε_{zz}^{pl} will be the "effective" macroscopic plastic deformations of the porous material.

Behavior of porous inverse opal material at significant deformation.

The study of significant deformations of a structure is dictated by the need to find critical values of the deformation of the material at which it will be considered destroyed or distorted sufficiently to represent a different structure than the one being studied. The criterion for the limit state of deformation was taken by us as the moment at which the opening between two pores was completely closed (Fig. 3). This criterion was chosen to track the magnitude of plastic deformations that lead to the transition of porosity from open to closed, that is, the moment when flow cannot occur between different points of the porous material. Moreover, depending on the porosity of the structure, the magnitude of the ultimate deformation is different. Thus, for a porosity of 56% (Fig. 3. a)) this deformation is about 30%, while for a porosity of 90% the deformation reaches about 70%.

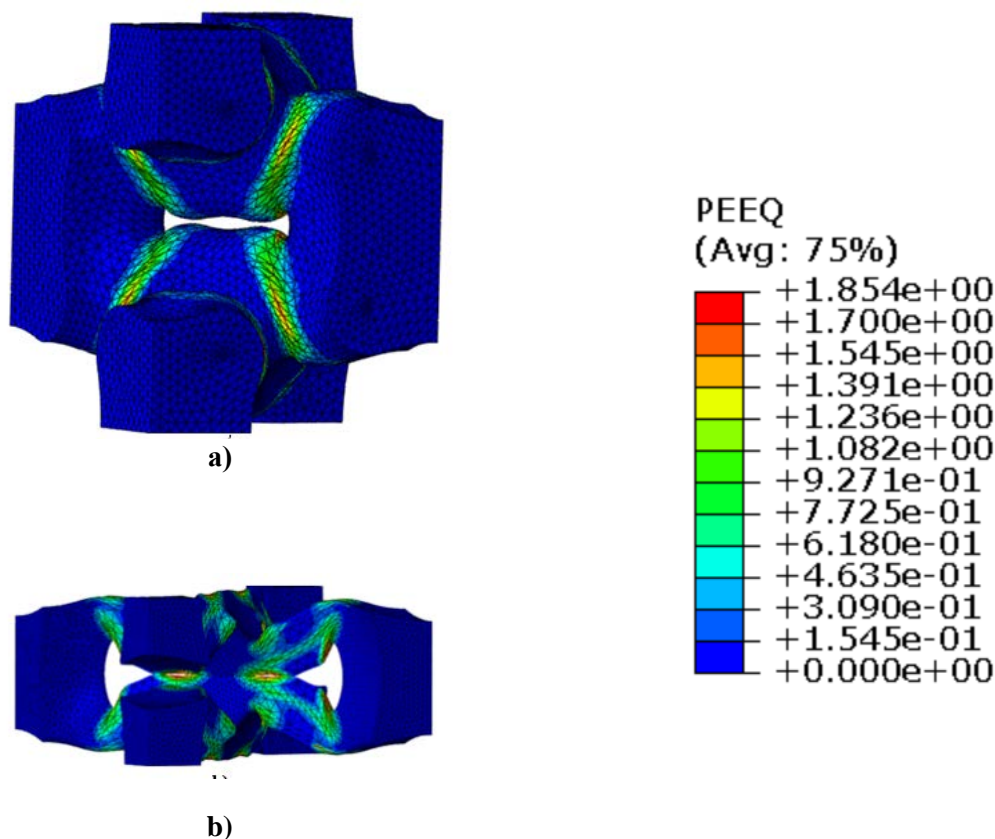


Fig.3. Accumulated strain of the structure: a) $\Theta=56,1\%$; b) $\Theta=90\%$

For the structure of inverse opal, we will show the dependence of the effective stress on deformation (Fig. 4). As can be seen from the graph, the deformation of the cell can be divided into three stages: a linear increase in stress to the value of the calculated yield strength $\sigma_{0,2}$, an inclined section of stress increase, and a horizontal section corresponding to the physical yield strength σ_T .

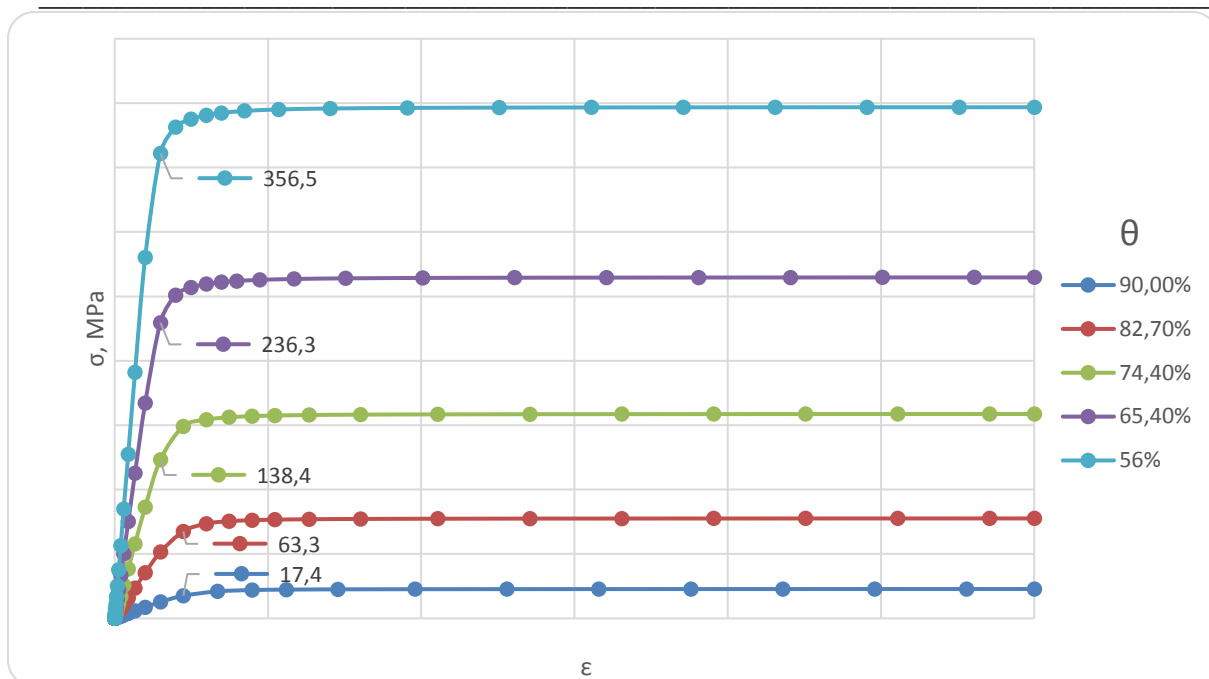


Fig.4. Dependence of effective stress on the degree of deformation for different porosities. The value of $\sigma_{0,2}$ is numerically indicated for each curve

It is important to note that the physical yield point σ_T for the inverse opal structure is higher than the engineering criterion $\sigma_{0,2}$. Moreover, with increasing porosity, this difference increases nonlinearly and for porosity 0.9 it reaches 31%.

At the first stage, elastic deformation of the cell occurs, which corresponds to the straight-line section of the graphs shown in Fig. 4. The geometry of the structure almost does not change, and stress concentration occurs at the transition points from the strut to the nodes of the inverse opal structure (Fig. 5).

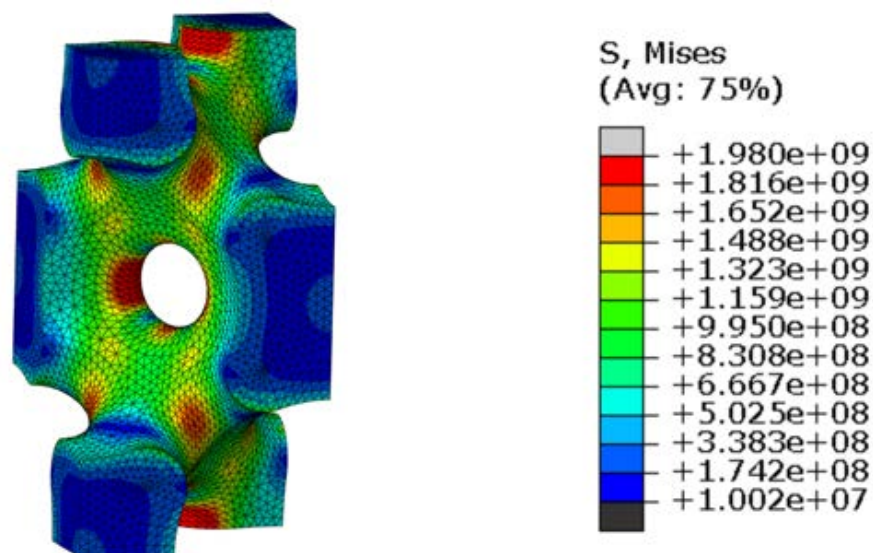


Fig.5. von Mises stress for the strain 1%, Pa

At the second stage, which corresponds to the nonlinear zone of the graph, the center of plastic deformation spreads (Fig. 6) in the volume of the solid phase material; it is in this area that the point corresponding to the residual deformation of 0.2% is located (the value of the yield strength $\sigma_{0,2}$ is shown as a footnote in Fig. 4). For this residual deformation, the total deformation value is from 1.4% to 2.2%.

depending on the porosity of the structure. In the second stage, plastic deformation occurs, which leads to a noticeable distortion of the structure, but the geometry itself remains characteristic of inverse opal.

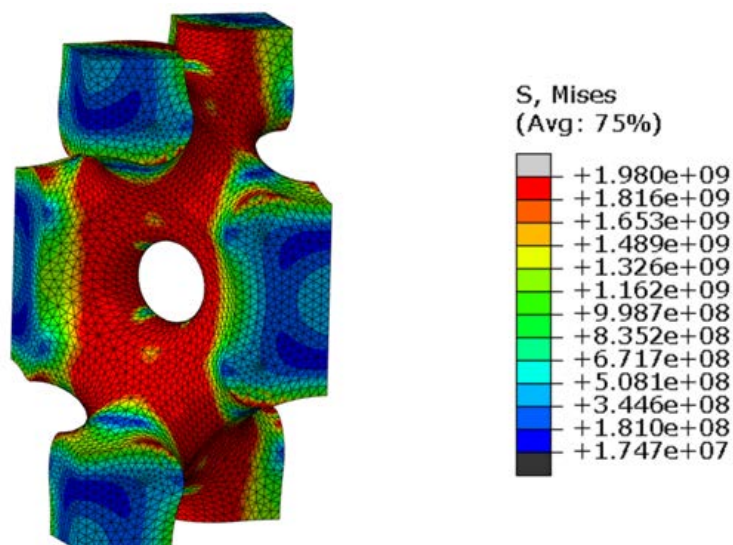


Fig.6. von Mises stress for the strain 1,5%, Pa

The third stage corresponds to the horizontal section of the graph - here the geometry of the structure undergoes significant distortions and mainly plastic bending of the struts connecting the nodes occurs for structures with high porosity, or approximate shear deformation along the rod cross-section for structures with medium porosity (Fig. 7).

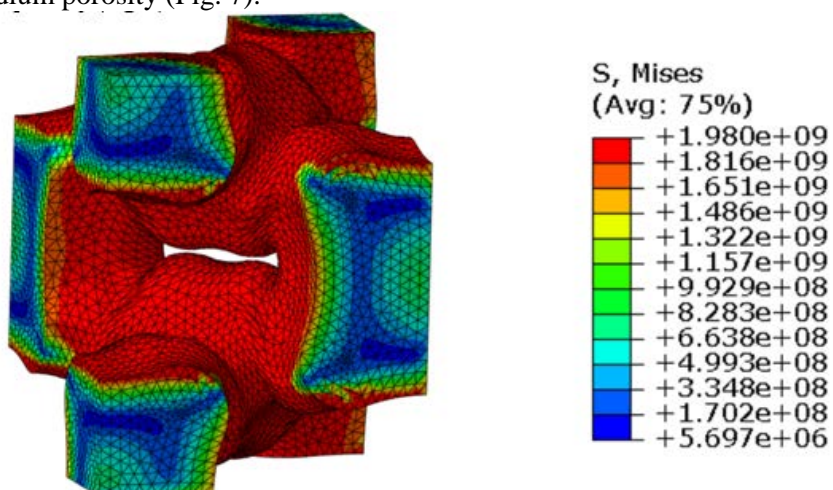


Fig.7. von Mises stress for the strain 30%, Pa

When the pore boundaries close, the effective behavior of the porous material begins to be variable resistance to tension-compression and possibly dilatant (non-zero average pressure under purely shear deformations and some volume growth under purely tangential stresses) [12].

Studying the behavior of the structure under significant deformations allows us to assess the technological qualities of the material in classical technologies of pressure processing of materials. Studying the issue of the critical value of the acquired deformation is also one of the main parameters for reproducing the material model in commercial application software packages. As shown above, the structure of inverse opal retains pore permeability at fairly high degrees of deformation.

Conclusions.

The process of irreversible plastic compression of a porous material with an inverse opal structure was simulated until the pore structure becomes almost completely closed. What is important for predicting the preservation of adsorption and chemical-catalytic functional properties of inverse opal materials during operation and pressure treatment. It was found that the structure of inverse opal retains open porosity even at relatively high degrees of deformation. The deformation value at which the contact of opposite parts of the pore surface occurs and the pore permeability is drastically reduced ranges from 0.3 for porosity 0.56

to 0.7 for porosity 0.9. It was also found that the physical yield point σ_T for the inverse opal structure is higher than the engineering criterion $\sigma_{0,2}$, and this tendency increases with increasing porosity, and for a porosity of 0.9 it reaches 31%. In addition, it was found that during uniform uniaxial compression of a porous inverse opal material, a significantly inhomogeneous stress-strain state is observed in the volume of a unit cell, so much so that in certain cases we can speak of localization of plastic flow of the base material.

References.

1. F. Capolino Theory and Phenomena of Metamaterials, CRC Press, 2017, 974 pp..
2. Pikul J.H., Özerinç S., Liu B., Zhang R., Braun P.V., Deshpande V.S., King W. P. High strength metallic wood from nanostructured nickel inverse opal materials. Scientific Reports 9, 719 (2019) <https://doi.org/10.1038/s41598-018-36901-3>
3. Rosario J.J., Berger J.B., Lilleodden E.T., McMeeking R.M., Schneider G.A. The stiffness and strength of metamaterials based on the inverse opal architecture. Extreme Mechanics Lett. 2016. Vol. 12. P. 86—96. <https://doi.org/10.1016/j.eml.2016.07.006>
4. Cao X., Wang Y., Wu X., Wang J., Ren H., Zhao Y. Multifunctional structural color Chinese herb hydrogel patches for wound management. Chemical Engineering Journal. 2024. Vol. 485, 149957 <https://doi.org/10.1016/j.cej.2024.149957>
5. Carroll A., Grant A., Zhang Y., Gulzar U., Douglas-Henry D., Nicolosi V., O'Dwyer C., The effect of TiO₂ and GeO₂ composite mixing on the behavior of macroporous Li-ion battery anode materials. J. Electrochemical Soc. 2023. Vol. 170. № 12. <https://doi.org/10.1149/1945-7111/ad1371>
6. Sandu I., Antohe I., Fleaca C.T., Dumitrache F., Urzica I., Brajnicov S., Iagaru R., Sava B., Dumitru M., Shaping in the third direction: self-assembly of convex colloidal photonic crystals on an optical fiber tip by hanging drop method. Polymers. 2024. Vol. 16(1), 33 <https://doi.org/10.3390/polym16010033>
7. Shuhang Lyu , Qianying Wu , Zheng Gong , et al. Thermomechanical Modeling and Stress Analysis of Copper Inverse Opals (CIO) Structure for Capillary-Fed Boiling. TechRxiv. December 04, 2023. <https://doi.org/10.36227/techrxiv.24654336.v1>
8. Коробко П.О., Кузьмов А.В. Ефективні пружні властивості пористих матеріалів зі структурою інверсного опалу. Наукові Нотатки. – 2024. – №77. – С. 46-50. <https://doi.org/10.36910/775.24153966.2024.77.7>
9. Korobko P.O., Kuzmov A.V. Effective Plastic Properties of Porous Materials with an Inverse Opal Structure. Powder Metall Met Ceram. – 2024. – Vol. 62. – Issue 9–10. <https://doi.org/10.1007/s11106-024-00418-4>
10. R. M. Christensen Mechanics of composite materials, , Wiley-Interscience, New York, 1979, 348 pp.
11. Bakhvalov N.S., Panasenko G.P. Homogenisation: Averaging processes in periodic media. Kluwer Academic Publishers, 1989. 366 pp.
12. Кузьмов А.В., Штерн М.Б., Коробко П.О. Моделювання впливу площинних дефектів на пластичність порошкових матеріалів обчислювальними методами мікромеханіки. Успіхи матеріалознавства. – 2021. – №3. – С. 77-85. <https://doi.org/10.15407/materials2021.03.077>

Рецензент: Вдовиченко Олександр Васильович, с.н.с., д.т.н., завідувач лабораторії акустичних методів дослідження матеріалів Інституту проблем матеріалознавства ім. І.М. Францевича НАН України.